

# A multi-directional backlight for a wide-angle, glasses-free three-dimensional display

David Fattal<sup>1</sup>, Zhen Peng<sup>1</sup>, Tho Tran<sup>1</sup>, Sonny Vo<sup>1</sup>, Marco Fiorentino<sup>1</sup>, Jim Brug<sup>1</sup> & Raymond G. Beausoleil<sup>1</sup>

Multiview three-dimensional (3D) displays can project the correct perspectives of a 3D image in many spatial directions simultaneously<sup>1–4</sup>. They provide a 3D stereoscopic experience to many viewers at the same time with full motion parallax and do not require special glasses or eye tracking. None of the leading multiview 3D solutions is particularly well suited to mobile devices (watches, mobile phones or tablets), which require the combination of a thin, portable form factor, a high spatial resolution and a wide full-parallax view zone (for short viewing distance from potentially steep angles). Here we introduce a multi-directional diffractive backlight technology that permits the rendering of high-resolution, full-parallax 3D images in a very wide view zone (up to 180 degrees in principle) at an observation distance of up to a metre. The key to our design is a guided-wave illumination technique based on light-emitting diodes that produces wide-angle multiview images in colour from a thin planar transparent light-guide. Pixels associated with different views or colours are spatially multiplexed and can be independently addressed and modulated at video rate using an external shutter plane. To illustrate the capabilities of this technology, we use simple ink masks or a high-resolution commercial liquid-crystal display unit to demonstrate passive and active (30 frames per second) modulation of a 64-view backlight, producing 3D images with a spatial resolution of 88 pixels per inch and full-motion parallax in an unprecedented view zone of 90 degrees. We also present several transparent hand-held prototypes showing animated sequences of up to six different 200-view images at a resolution of 127 pixels per inch.

Ideally, a perfect 3D display would reproduce the set of all light rays (or lightfield<sup>5</sup>) from a 3D scene. Although standard holography can perform this task very well, the recording of a holographic medium is too slow to permit real-time operation<sup>6</sup>. Autostereoscopic multiview 3D displays are ‘the next-best thing’: they discretize the lightfield into narrowly spaced views to create the illusion of continuous parallax and a 3D stereoscopic effect up to a certain viewing distance<sup>1,2</sup>. They can be realized using pure geometrical optics techniques such as multi-projector<sup>7</sup>, parallax barrier<sup>3</sup>, integral imaging<sup>8</sup> or a combination of these<sup>4,9</sup>. Multi-projector solutions have demonstrated impressively large 3D images with many views and high resolution, but they are difficult to implement on a mobile device. Recent lenticular-based solutions (see <http://www.alioscopy.com> and <http://www.dimencodisplays.com>) have seemed promising for TV applications owing to their compatibility with standard liquid-crystal displays (LCDs); however, they provide only a limited amount of head movement (with the sets of views repeating several times across the view zone), and low resolution.

Diffractive optics offers another way of creating a multiview lightfield. Digital holographic displays use a spatial light modulator to update small holographic cells (sometimes called hogels<sup>10</sup>), each generating a few light rays. Despite recent progress (<http://www.zebraimaging.com>), the required density of active pixels limits the field of view (FOV) and precludes the operation of the digital holographic displays at video rate. Using a static fringe pattern with an external modulator<sup>11</sup> can solve the video rate problem for a more modest number of views. Still, because

those diffractive approaches rely on the first-order diffraction of a highly collimated free-space light source, they are hard to integrate, have limited power efficiency, and are plagued by the presence of specular light and unwanted diffraction orders (even for complex diffractive elements such as blazed or sub-wavelength gratings<sup>12</sup>).

Here we introduce a diffractive backlight solution that seems well suited to realizing a multiview 3D display for mobile devices. It features (1) full motion parallax in a wide view zone (90° FOV demonstrated), (2) static ‘directional pixels’ (binary diffraction gratings) that can be manufactured at low cost and individually modulated at video rate, and (3) edge lighting by standard light-emitting diode (LED) light with a compact collimation system. In addition, it can render colour without the need for colour filters, allowing full transparency of the display (with transparent electronics).

The cornerstone of our display architecture is a set of directional grating pixels shown schematically in Fig. 1. The gratings are etched or deposited on the backlight surface, and illuminated by collimated light that is guided in the backlight substrate by total internal reflection. As a result of first-order diffraction, light with input planar momentum  $k_{\text{in}} = (n_{\text{eff}}, 0, 0)2\pi/\lambda$  is scattered out of the backlight in a well-defined direction characterized by the normalized output vector  $k_{\text{out}} = (n_x, n_y, n_z)2\pi/\lambda$ , where:

$$n_x = n_{\text{eff}} - (\lambda/\Lambda)\cos\phi \quad (1)$$

$$n_y = -(\lambda/\Lambda)\sin\phi \quad (2)$$

Also,  $n_x^2 + n_y^2 + n_z^2 = 1$ ,  $n_{\text{eff}}$  is the effective index of propagation of the input light along the  $x$  axis,  $\Lambda$  is the grating pitch and  $\phi$  is the groove orientation with respect to the  $y$  axis. A group of directional gratings covering all views in the FOV forms a multiview pixel—the basic unit cell of our backlight.

The guided nature of the input light ( $n_{\text{eff}} > 1$ ) completely suppresses specular light in the FOV. It also repels higher diffraction orders away from the display normal, ensuring a wide view zone free of ghost images. In the Supplementary Information, we prove that the extent of the ‘clean’ view zone (measured in terms of the angle  $\alpha$  from the vertical axis ( $z$  axis) is:

$$\sin\alpha = n_{\text{eff}}/2 \quad (3)$$

For a glass or plastic backlight, this corresponds to a FOV ( $2\alpha$ ) of 90° (and a high-refractive-index glass<sup>13</sup> could be used to reach an FOV close to 180°). The guided light illumination is essential for another reason: it allows spatial multiplexing of three pixel sets that can be selectively addressed by changing the illumination angle. This important feature allows the spatial multiplexing of colour without using colour filters, potentially increasing the power efficiency and enabling a completely transparent architecture. This illumination technique

<sup>1</sup>Hewlett-Packard Laboratories, 1501 Page Mill Road, Palo Alto, California 94304, USA.

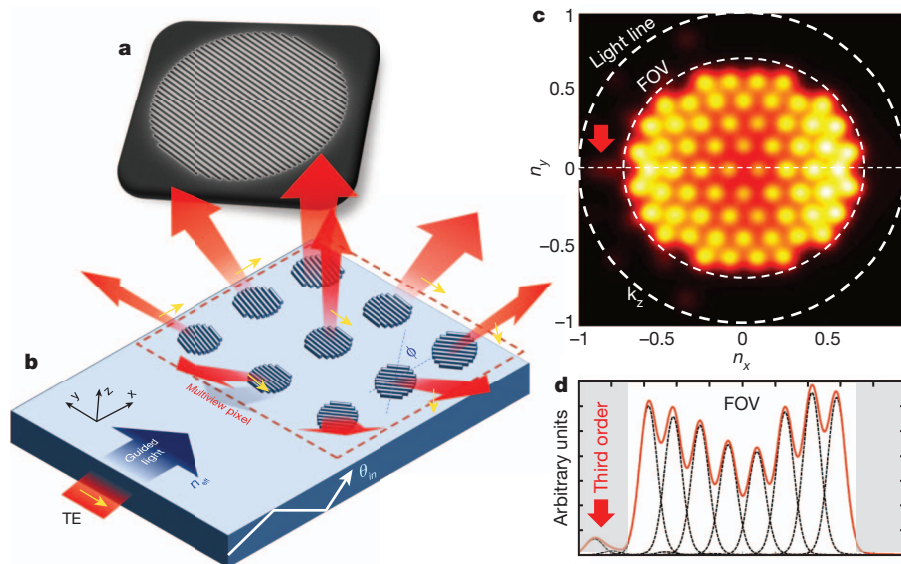


**Figure 1 | Multi-directional backlight concept.** **a**, Scanning electron micrograph of grating pixel fabricated by conventional photolithography. **b**, Schematic of the multi-directional backlight under collimated light illumination. ‘Directional’ grating pixels scatter the input light into the view zone of the display by first-order diffraction. Owing to the large planar momentum of the input light, unwanted diffraction orders fall far from the display normal. Under illumination by TE (transverse electric) polarized light, the output polarization is well preserved, which facilitates the external modulation of the backlight using commercial liquid-crystal technology.  $\theta_{in}$ ,

the angle of propagation of the input light in the backlight, with respect to the horizontal plane. **c**, Full-wave simulation of the radiation pattern from a 64-view backlight with 12- $\mu\text{m}$ -diameter red grating pixels under illumination by a collimated LED light source (20 nm spectral width,  $\pm 3.5^\circ$  collimation approximating our experimental lighting conditions). The upward flux is  $k_z|E|^2$ . **d**, Cross-section of **c** along the horizontal axis with individual view contributions (dotted black lines). The diffraction efficiency for each view is about 5% for 100-nm-deep grating grooves. The red arrow indicates the presence of a third-order diffracted beam outside the FOV.

also allows us to create animated sequences of 3D images in a very simple way.

The use of diffractive pixels allows us to define almost arbitrary spatio-angular characteristics for the emitted lightfield. For example, we can increase the angular density near the normal direction and decrease it at sharper view angles. We can increase the number of horizontal views and reduce the number of vertical views. We can adopt a hexagonal angular grid (as in Fig. 1c) to obtain more uniform transitions between views, allowing us to control the amount of between-view leakage and angular aliasing<sup>14,15</sup>. More importantly, it permits us to mix standard, non-directional pixels (implemented as chirped broadband gratings) with directional pixels on the backlight surface to enable high-definition two-dimensional 2D content and lower-resolution 3D content simultaneously.

The visual experience provided by a multiview 3D display can be characterized by its spatial resolution (multiview pixel size  $p$ ), and angular resolution (between-view distance  $\Delta\theta$ ), or number of views  $N = (2\sin\alpha/\Delta\theta)^2$ . The maximum distance at which the stereo effect can be continuously perceived in the FOV is  $z_{3D} \approx 6.3 \text{ cm}/\Delta\theta$ , where 6.3 cm is the average human eye separation<sup>16</sup>. The depth of field ( $p/\Delta\theta$ ) measures the maximum altitude of an image that can be displayed at the native resolution  $p$  of the display with a disparity of less than one pixel between neighbouring views (larger disparity content will show

some blurring and ‘jumps’ between views<sup>15</sup>). The effective resolution at height  $z$  (where  $z = 0$  is the surface of the display) is  $p_{\text{eff}}(z) = \max(p, z\Delta\theta)$ . The maximum number of views that our backlight can accommodate is:

$$N \approx p\sin\alpha/(\lambda\beta\sqrt{n}) \quad (4)$$

where  $n$  is the number of spatially multiplexed pixel sets ( $n = 3$  for a red–green–blue (RGB) backlight) and  $\beta$  is a geometrical factor that depends on the spatio-angular pixel layout ( $\beta = 1.22$  for a close-packed square array of circular pixels, with a hexagonal distribution of views within the FOV and between-view separation corresponding to one Rayleigh width). Table 1 illustrates the imaging performance of a full-colour backlight with  $90^\circ$  FOV for various pixel sizes. The backlight can be improved by incorporating a set of ‘broadband’ pixels to increase the resolution of low-disparity content without decreasing the depth of field, or by using time-multiplexing schemes to increase the effective view number. Such refinements will be the topic of future study.

In practice, the angular divergence of the views is broadened beyond the diffraction limit by the finite spectral and angular distribution of the input light. Figure 1c and d presents the simulated radiation pattern<sup>17</sup> of our 64-view backlight prototype, designed with an FOV of  $90^\circ$  and inter-view separation  $\theta$  of  $10^\circ$  to accommodate an input-beam spectral width of 20 nm and angular width of  $\pm 3.5^\circ$ . The brightness variation across the FOV (centred around a diffraction efficiency of 5%

**Table 1 | Theoretical characteristics of diffraction-limited backlight**

3D imaging characteristics of a full-colour backlight	Diffraction-limited performance*			64-view experimental backlight of Fig. 1c and d
Multiview pixel size, $p$ (mm)	0.25	0.5	1.0	0.288
Number of views per colour, $N$	133	266	531	64
Angular separation between views, $\Delta\theta$ ( $^\circ$ )	7.0	5.0	3.5	10
Diameter of each grating sub-pixel, $D$ ( $\mu\text{m}$ )	12.5	17.7	25.1	12
Stereo distance, $z_{3D}$ (cm)	51	73	103	36
Depth of field (mm)	2.0	5.8	16.3	1.7
Effective resolution at height 2 cm, $p_{\text{eff}}$ (mm)	2.5	1.7	1.2	3.5

\* Shown are three distinct designs with increasing pixel size, highlighting the trade-off between spatial resolution (pixel size  $p$ ) and angular resolution (angular separation  $\Delta\theta$ ).

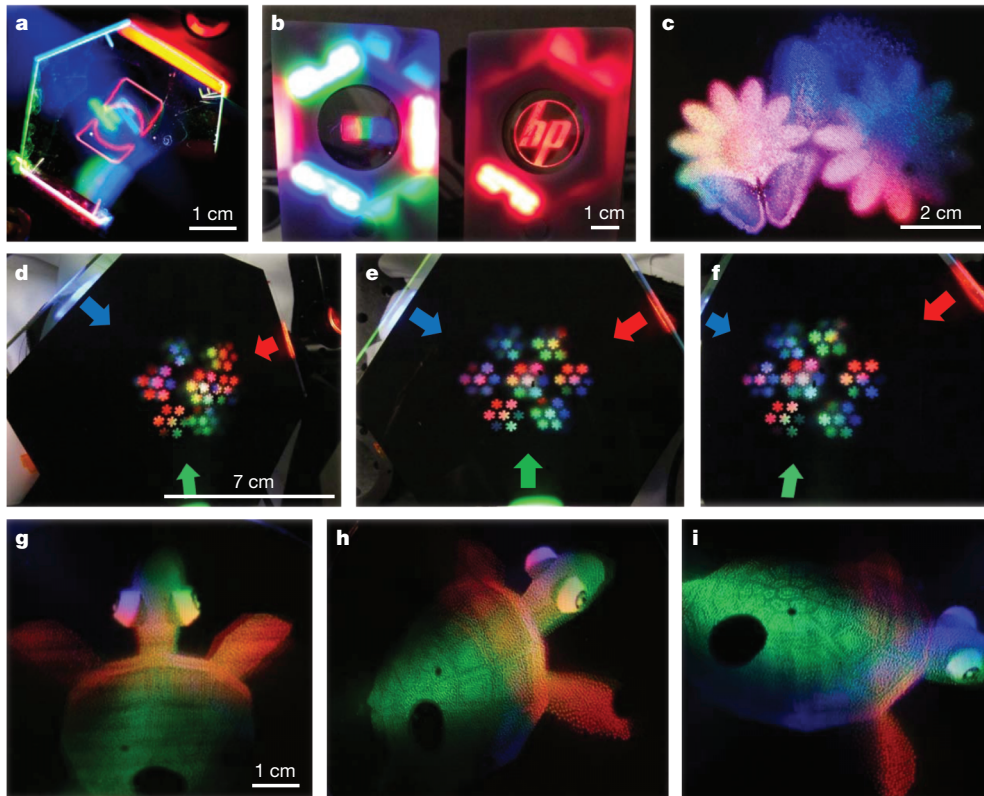


**Figure 2 | 3D images from a passively modulated backlight.** **a, b,** Portable, transparent backlight prototype, with resolution 127 pixels per inch, 200 views, wide view zone of  $90^\circ$  (full parallax). The red HP logo in **b** is animated in a 'breathing' motion by periodically cycling through one of six LED arrays (see Supplementary Video). **c,** Colour dithered 3D image obtained by masking dark pixels from a fully covered backlight, using a high-resolution ink-printed

pattern. **d–f,** Steep angle views from the same backlight as **c** with a test pattern (colour 'snow flakes') showing 4 cm of rendered depth and colour mixing. Scale bar in **d** refers to **e** and **f** as well; scale bar in **g** refers to **h** and **i** as well. We note that the elements of the image with highest disparity (located at  $z = 2$  cm) show some blurring, owing to the engineered view overlap of the backlight. **g–i,** Turtle 3D image viewed from various viewpoints.

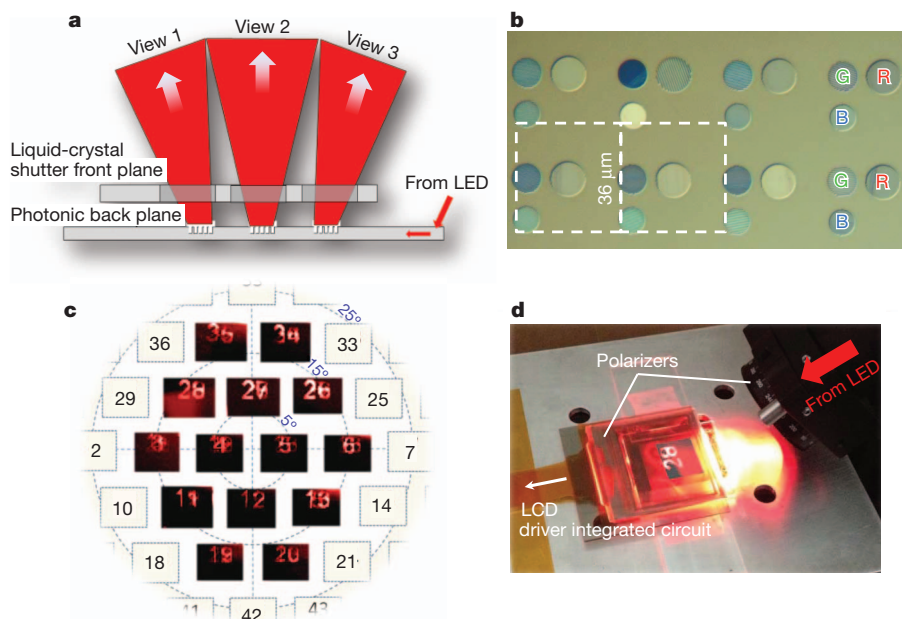


**Figure 3 | Actively modulated backlight.** **a,** Schematics of a side-illuminated backlight actively modulated by an LCD shutter plane. The shutter plane must be located close enough to the backlight surface to avoid beam walk-off. **b,** Optical microscope image of the pixel arrangement on the backlight surface. Although all three RGB pixels were present on the backlight, we used only the red pixels for that prototype. The dotted white squares indicate the alignment of the liquid-crystal cell with respect to the pixel array. **c,** Multiview image

showing a different number in different view zones. Images corresponding to neighbouring views 'bleed' into each other owing to the designed view overlap, introduced to smooth out between-view transitions. **d,** Global view of the LCD modulated prototype. Red light from an external LED is expanded and collimated using free-space optics elements, and linearly polarized before it enters the backlight directly from a polished edge. The LCD shutter plane was thinned to  $50\ \mu\text{m}$  and aligned to the pixel array with an accuracy of about  $2\ \mu\text{m}$ .

for light diffracted above the grating, for 100-nm grating grooves) and the predicted view divergence (about  $6.5^\circ$  full width at half maximum, FWHM) compare well with the data reported in the Supplementary Information.

We present a series of prototypes of increased complexity to showcase the features of our backlight technology. We fabricate hand-held devices featuring a transparent backlight with partial pixel coverage, able to project static 3D RGB images or animated sequences of up to six monochrome 3D images ( $90^\circ$  FOV, 200  $\mu\text{m}$  resolution, 200 views per colour; see Fig. 2a and b). We also fabricate several 6-inch backlights with full pixel coverage (see Fig. 1c and d), on which we overlaid high-resolution binary masking patterns (ink on plastic from a high-resolution printer) to create larger 64-view images with colour mixing and dithering (Fig. 2c–i).

Finally, we use the front plane of a Sony LCD pico-projector to modulate a 1-inch 64-view backlight at a rate of 30 frames per second. As shown in Fig. 3, the backlight contains a 720 by 720 array of grating pixels, with a pitch of 36  $\mu\text{m}$ . Because the gratings in the backlight do not significantly change the polarization of horizontally (transverse electric) polarized light, only the output polarizer is needed for the LCD. Figure 3d shows a multiview image created by the LCD in which each view displays a different number from 1 to 64. To avoid ‘beam walk-off’ from the grating pixels to their respective liquid-crystal cell, the top glass cover needs to be thinned to about 20  $\mu\text{m}$ . The resulting devices were not strong enough for extensive testing, so here we report the operation of a stable device featuring a LCD cover thickness of about 50  $\mu\text{m}$ , allowing the modulation of 14 of the original 64 views (the unmodulated views are greyed out on Fig. 3d). The pictures taken of the 14 central views show a small amount of between-view mixing, in qualitative agreement with the simulation of Fig. 1c and d. At the centre of views 12 or 28, for instance, no leakage from neighbouring views is discernible. In view 27, the view point leans towards view 26 and the between-view leakage is apparent. See the Supplementary Information for videos of all static and active demonstrations.

Our multi-directional backlight provides the basis for a very efficient display, because it does not require colour filters, and can use multiple passes of the incident light, much as in a standard LCD. In its present form, the intensity of the input light decreases from the edge to the centre, which can be compensated in a variety of ways (for example, by adjusting scattering strength via groove depth or area variation). We are currently working on other pixel modulation methods that do not require polarized light and should increase the efficiency even further.

We believe that the unique combination of wide-angle 3D performance, high spatial resolution, ease of modulation at video rate, compact form factor and low manufacturing cost make our multi-directional backlight technology very promising for multiview 3D mobile display applications.

## METHODS SUMMARY

The glass backlight prototypes presented in this paper are made of Schott glass B270, covered by a 100-nm layer of silicon nitride fabricated by plasma-enhanced chemical vapour deposition. Some of the static images were defined by electron-beam lithography using a 200-nm PMMA photoresist layer covered by 2 nm of

evaporated chrome. The nitride layer was etched in an Oxford reactive ion etching system using chlorine chemistry. The  $720 \times 720$  grating pixel array for the LCD modulated backlight was defined by a 193-nm deep-ultraviolet photolithography process. The finite-difference time domain simulations were performed on a Hewlett-Packard-owned computer cluster using the parallel version of MEEP<sup>17</sup> with 256 simultaneous cores.

Received 12 October 2012; accepted 30 January 2013.

1. Dodgson, N. Autostereoscopic 3D displays. *Computer* **38**, 31–36 (2005).
2. Okoshi, T. *Three-Dimensional Imaging Techniques* (Atara Press, 2011).
3. Wetzstein, G., Lanman, D., Heidrich, W. & Raskar, R. Layered 3D: tomographic image synthesis for attenuation-based light field and high dynamic range displays. *ACM Trans. Graph.* **30** (95), 1–12 (2011).
4. Wetzstein, G., Lanman, D., Hirsch, M. & Raskar, R. Tensor displays: compressive light field synthesis using multilayer displays with directional backlighting. *ACM Trans. Graph. (Proc. SIGGRAPH)* **31**, 1–11 (2012).
5. Levoy, M. & Hanrahan, P. Light field rendering. In *Proc. 23rd Ann. Conf. on Computer Graphics And Interactive Techniques (SIGGRAPH '96)* 31–42 (ACM, New York, 1996).
6. Blanche, P. A. et al. Holographic three-dimensional telepresence using large-area photorefractive polymer. *Nature* **468**, 80–83 (2010).
7. Kawakita, M. et al. 3D image quality of 200-inch glasses-free 3D display system. *Proc. SPIE* **8288**, <http://dx.doi.org/10.1117/12.912274> (2012).
8. van Berkel, C. & Clarke, J. A. Characterization and optimization of 3D-LCD module design. *Proc. SPIE* **3012**, 179–186 (1997).
9. Takaki, Y. & Nago, N. Multi-projection of lenticular displays to construct a 256-view super multi-view display. *Opt. Express* **18**, 8824–8835 (2010).
10. Lucente, M. *Diffraction-Specific Fringe Computation for Electro-Holography*. PhD thesis (MIT, 1994).
11. Kulick, J. H. et al. Partial pixels: a three-dimensional diffractive display architecture. *J. Opt. Soc. Am. A* **12**, 73–83 (1995).
12. Astilean, S., Lalanne, P., Chavel, P., Cambriel, E. & Launois, H. High-efficiency sub-wavelength diffractive element patterned in a high-refractive-index material for 633 nm. *Opt. Lett.* **23**, 552–554 (1998).
13. Fu, J. Optical glass. US patent 8,187 986 (2012).
14. Ramachandra, V., Hirakawa, K., Zwicker, M. & Nguyen, T. Spatioangular prefiltering for multiview 3D displays. *IEEE Trans. Vis. Comput. Graph.* **17**, 642–654 (2011).
15. Zwicker, M., Matusik, W., Durand, F. & Pfister, H. Antialiasing for automultiscopic 3D displays. In *Eurographics Symposium on Rendering* (2006).
16. Dodgson, N. A. Variation and extrema of human interpupillary distance. *Proc. SPIE* **5291**, 36–46 (2004).
17. Oskooi, A. F. et al. MEEP: a flexible free-software package for electromagnetic simulations by the FDTD method. *Comp. Phys. Commun.* **181**, 687–702 (2010).

Supplementary Information is available in the online version of the paper.

**Acknowledgements** We are grateful to C. Santori for many suggestions on the backlight design, A. Jeans for performing the roll-to-roll imprint jobs, A. Said for generating some of the multiview images shown in Fig. 2, L. Kiyama and W. Mack for the printed circuit board design of the portable prototypes, R. Cobene for his help with packaging, P. Beck for her help in the cleanroom, and B. Culbertson and C. Patel for their support of the project.

**Author Contributions** All authors contributed extensively to the work presented in this paper. D.F. conceived the multi-directional backlight concept. D.F. and J.B. led the technical effort to realize the various prototypes. D.F., Z.P., S.V. and T.T. were responsible for the nanometre-scale fabrication of the backlight. J.B. and M.F. were responsible for the optical design and assembly of the prototypes. M.F. designed the illumination systems and part of the other electronics for the prototypes. R.G.B. supervised and coordinated the project. All authors contributed to the data analysis. D.F. and R.G.B. prepared the manuscript with input from J.B., M.F. and Z.P.

**Author Information** Reprints and permissions information is available at [www.nature.com/reprints](http://www.nature.com/reprints). The authors declare no competing financial interests. Readers are welcome to comment on the online version of the paper. Correspondence and requests for materials should be addressed to D.F. ([david.fattal@hp.com](mailto:david.fattal@hp.com)).